

5 December 1998

Light Yield Measurement of the 1998 Tile Barrel Module0 using muon beams

S. Němeček

Institute of Physics of ASCR, Praha, Czech Republic

T. Davídek, R. Leitner

Faculty of Math. and Phys., Charles University, Praha, Czech Republic

ATL-TILECAL-99-003

1 Feb 1999



Abstract

The light yield for each cell of the Tile barrel Module 0 was measured using 1998 test beam data. Six data sets of muon beams at 90 degrees entering the different tiles centres were analysed.

Standard technique of photoelectron statistics evaluation from signals of two photo-tubes optically connected to the same cell was improved by splitting the response spectrum into several slices.

The mean values of (41, 49, 53) and (43, 43, 47) photoelectrons per GeV per cell have been measured for the three radial samplings and for the two halves of the Module 0 read-out by different WLS fibres. The differences are discussed in the text.

The measured numbers are sufficiently large not to influence the calorimeter resolution. The best value of 53 photoelectrons per GeV per cell is close to the best value of 64 photoelectrons per GeV per cell measured for the 1995 TileCal prototypes.

1 Introduction

Newly instrumented Module 0 of the ATLAS barrel tile calorimeter[1] was tested in H8 beam of the CERN SPS accelerator in June - July 1998.

The same mechanical structure, as used in the 1996 Tilecal barrel Module 0 beam tests, was equipped with a new batch of scintillators and with different types of WLS fibres from Pol.Hi.Tech (the positive η side) and from Bicron (the negative η side).

To study the influence of the UV absorber (UVA) the Bicron multicladd fibres BCF99-28 with 60 ppm of UVA were used for about one fifth of the longitudinal calorimeter depth (Sampling A), while the Bicron BCF91A multicladd fibres without UVA were used for the rest of the negative η side of Module 0.

The light output and non-uniformity within a cell and between cells are important characteristics of the calorimeter. Muon beams entering the different tiles centres at 90 degrees are a suitable tool to test the optical system, producing light along the whole path through the calorimeter structure.

One half of the symmetrical Tilecal cell structure is shown on Fig. 1.

Eleven sets of tiles of different radial sizes form the longitudinal segmentation of detector. A pair of WLS fibres running radially collect light from the tiles on both their ϕ edges.

Each cell contains several tile sizes depending on radial depth, namely 3 tiles (Size No. 1 to 3) in sampling A, 6 tiles (Size No. 4 to 9) in sampling B and 2 tiles (Size No. 10 and 11) in sampling D.

2 The Data

During the 1998 test beam period the electronic channels for only half of the module were available. Therefore, the samplings A, B and D were read either on the negative or positive η side. The first four data sets marked as JUL10, JUL11, JUL12odd and JUL12even were taken with these conditions.

For a part of the test beam, the electronic channels were rearranged to read at the same time both the positive and negative η sides for sampling B. The

corresponding data samples are denoted as JUL+17 and JUL-17 resp. JUL+20 and JUL-20.

The PMT response was checked in each run, the reconstructed charge could be compared on Fig. 2 for fired and non fired PMT. Only one channel (PMT 28) for data from 12-th July did not work and the corresponding cell B4 in data sets JUL12even and JUL12odd was excluded from the analysis.

3 The Method

The standard technique[3] of estimating the number of photoelectrons ($N_{p.e.}$) from the difference and the sum of the anode charge in two photo-tubes simultaneously seeing the same light source was improved. To relate the $N_{p.e.}$ determination to the fixed amount of light coming to the photo-tubes and to minimalise the influence of fluctuations of muon energy loss governed by Landau distribution, the resulting charge spectrum of two photo-tubes seeing the same cell was sliced into several intervals. In each interval, the mean value of the sum S_{L+R} of responses of the two PMTs has been evaluated as well as the sigma σ_{L-R} of the Gaussian distribution of the difference of the two signals. The measured variables are connected by the relation:

$$\sigma_{L-R}^2 = \frac{C}{N_{p.e.}} \cdot S_{L+R} + \sigma_0^2,$$

where the factor to correct for statistical fluctuations in the first few dynodes, $C = 1.11$, was taken following Ref.[2].

Both variables S_{L+R} and σ_{L-R} are expressed in GeV. The conversion coefficient between pC and GeV for 180 GeV muons, the only muon beam energy used, was obtained from two factors. The first factor is the value found using electron data ($1 \text{ GeV} = 0.85 \text{ pC}$), the second is the factor $\frac{\epsilon}{\mu}$ relating the electron and muon energy losses. The value $\frac{\epsilon}{\mu} = 0.91$ measured [3] for the tile calorimeter prototype was used. $N_{p.e.}$ is then a number of photoelectrons per 1 GeV of energy deposited in a cell. The parameter σ_0^2 , corresponding to a noise, is very small and was neglected, consequently the $N_{p.e.}$ was slightly underestimated. The increase of the number of photoelectrons per cell by taking into account a noise term was found to be $(4.3 \pm 1.7)\%$ for the JUL10 data set.

The method is illustrated in Fig. 3, where the slices are depicted on the spectrum of the muon energy loss in the cell D3. Fig. 4 shows the fit of $N_{p.e.}$ for the cell B9

together with the number of events in each slice. The numbers obtained by this method agree well with previously used method for $N_{p.e.}$ measurement based on the truncated muon response spectrum.

4 Results

The number of photoelectrons ($N_{p.e.}$) calculated for each cell and then averaged over all cells that muons pass through in a given run is shown in Fig. 5 for all different tile sizes. All pairs of data sets give the same results at the 3% level.

The average $N_{p.e.}$ of the cells within the same sampling are listed in Table 1 and on Fig. 5 and Fig. 6. The spread, at level of 3 to 9% is caused mainly by cell to cell fluctuations within the corresponding sampling.

5 Conclusions

For each tile of sampling B, the $N_{p.e.}$ in the cell of the positive η side (equipped by Pol.Hi.Tech fibres S250 with double cladding), was compared to the $N_{p.e.}$ in the cell of the negative η side (equipped by Bicon fibres BCF91A multicladd fibres without UVA). The measured ratio ($89 \pm 7\%$) may be interpreted as about 10% higher light output of the Bicon fibres. The $N_{p.e.}$ of sampling B, averaged over all four data sets, is 48 and 42 photoelectrons for Bicon and Pol.Hi.Tech fibres, respectively. A similar difference was measured in sampling D.

It should be noticed, however, that negative and positive η sides were read-out by PMTs of two different series. The $N_{p.e.}$ is a product:

$$N_{p.e.} = N_{photons}(tiles, fibres) \cdot Q.E.(PMT),$$

of the number of photons $N_{photons}$ which reach the PMT's photocatode and of the quantum efficiency $Q.E.(PMT)$ of the PMT's. Therefore the conclusions drawn above are valid only under the assumption, that the quantum efficiencies of PMT's are the same for the two series.

The difference of light yield between sampling A and B on the negative η side could be explained by larger light attenuation in fibres doped by UV absorber

	Negative η (Bicron)				Positive η (Pol.Hi.Tech)			
	JUL10		JUL11		JUL12odd		JUL12even	
	$\langle N_{p.e.} \rangle$	RMS	$\langle N_{p.e.} \rangle$	RMS	$\langle N_{p.e.} \rangle$	RMS	$\langle N_{p.e.} \rangle$	RMS
Sampling D	52.7	3.7	52.7	3.4	48.3	2.2	46.3	1.5
Sampling B	48.9	3.2	49.1	3.3	42.5	3.8	42.8	3.5
Sampling A	41.2	2.7	40.7	3.1	42.6	3.2	42.9	2.8

	JUL-17		JUL-20		JUL+17		JUL+20	
	$\langle N_{p.e.} \rangle$	RMS	$\langle N_{p.e.} \rangle$	RMS	$\langle N_{p.e.} \rangle$	RMS	$\langle N_{p.e.} \rangle$	RMS
Sampling B	47.2	3.0	47.9	3.4	41.4	3.0	42.2	3.2

Table 1: The number of photoelectrons per 1 GeV per cell averaged over all cells and over all tile sizes in a given sampling either on positive or on negative η side of the Module 0. The $\langle N_{p.e.} \rangle$ of sampling B averaged over all four data sets is 48 and 42 photoelectrons for Bicron and Pol.Hi.Tech fibres respectively. The difference of light yield between sampling A and B on the negative η side could be explained by larger light attenuation in fibres doped by UV absorber (UVA).

(UVA). The ratio of cell responses in sampling A divided by ones in sampling B for the JUL11 data set gives 83% with spread of 7% .

6 Acknowledgements

Financial support of Prague group by grant project RP-4210/69/98 of the Ministry of Industry and Trade of the Czech Republic.

References

- [1] ATLAS Tile Calorimeter Technical Design Report, CERN/LHCC/96-42 ATLAS TDR 3.
- [2] A. Bernstein *et al.*, Nucl. Instr. and Meth. **A336** (1993) 23. A. Bernstein *et al.*, Nucl. Instr. and Meth. **A262** (1987) 229.
- [3] Z. Ajaltouni *et al.*, Nucl. Instr. and Meth. **A388** (1997) 64.
- [4] T. Davidek and R. Leitner: *Parametrization of the Muon Response in the Tile Calorimeter* ATLAS internal note, TILECAL-NO-114, 5 March 1997

TILECAL CELLS

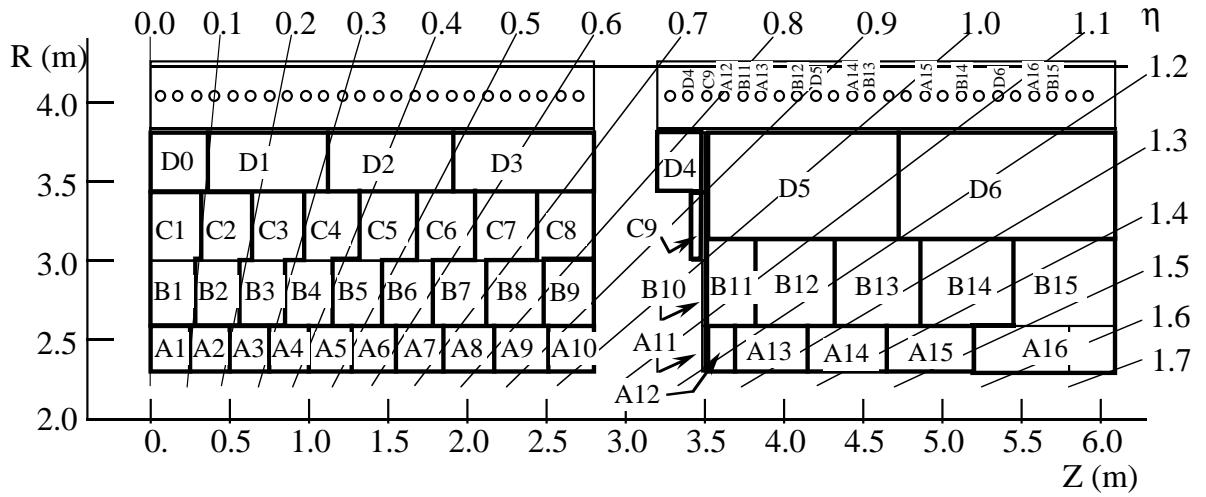


Figure 1: The figure shows the barrel and extended barrel sections of the Tile Calorimeter. Signals from the scintillators are grouped into the rectangular cells shown and each cell is viewed by a pair of photomultipliers (called L and R in the tables below). In the barrel section, cells B_i and C_i are viewed by the same pair of photomultipliers. The cell dimensions are chosen to obtain pseudo-projective towers of nominal width $\Delta\eta = 0.1$.

Data set JUL12even

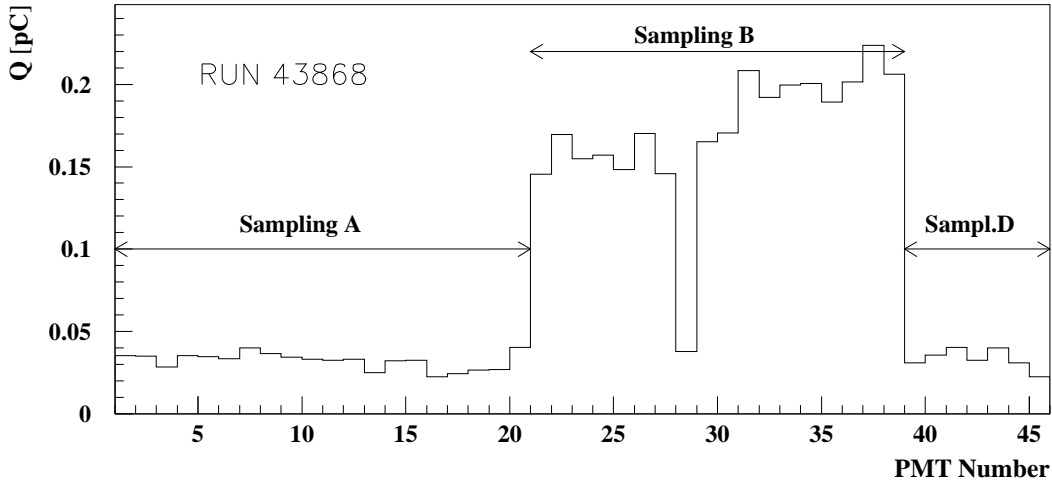


Figure 2: The reconstructed anode charge for each of the 45 photo-tubes connected to the DAQ in this RUN, when the muon beam enters at 90 degrees at the centre of Tile size 4 and passes through cells B9, B8,..., up to B1, PMTs No.21 to No.38 should give a signal. This is the case except for PMT No.28, the upper one of cell B4. This cell was therefore excluded from $N_{p.e.}$ calculation.

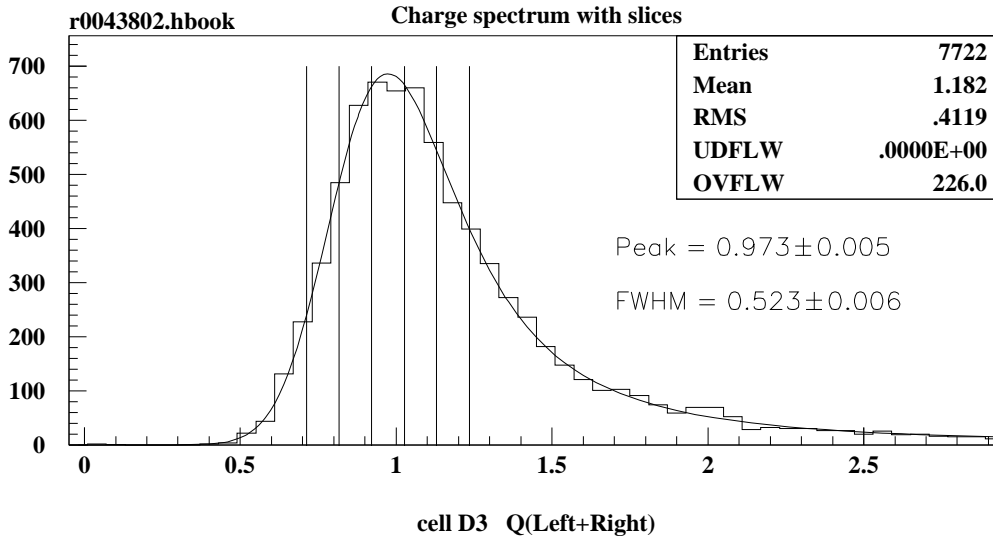


Figure 3: The spectrum of the sum S_{L+R} of PMT anode charges corresponding to muon energy loss in the cell D3, with a fit to a Gauss-Landau convolution[4]. The slices used for the $N_{p.e.}$ calculation by the method described in this Note are also depicted.

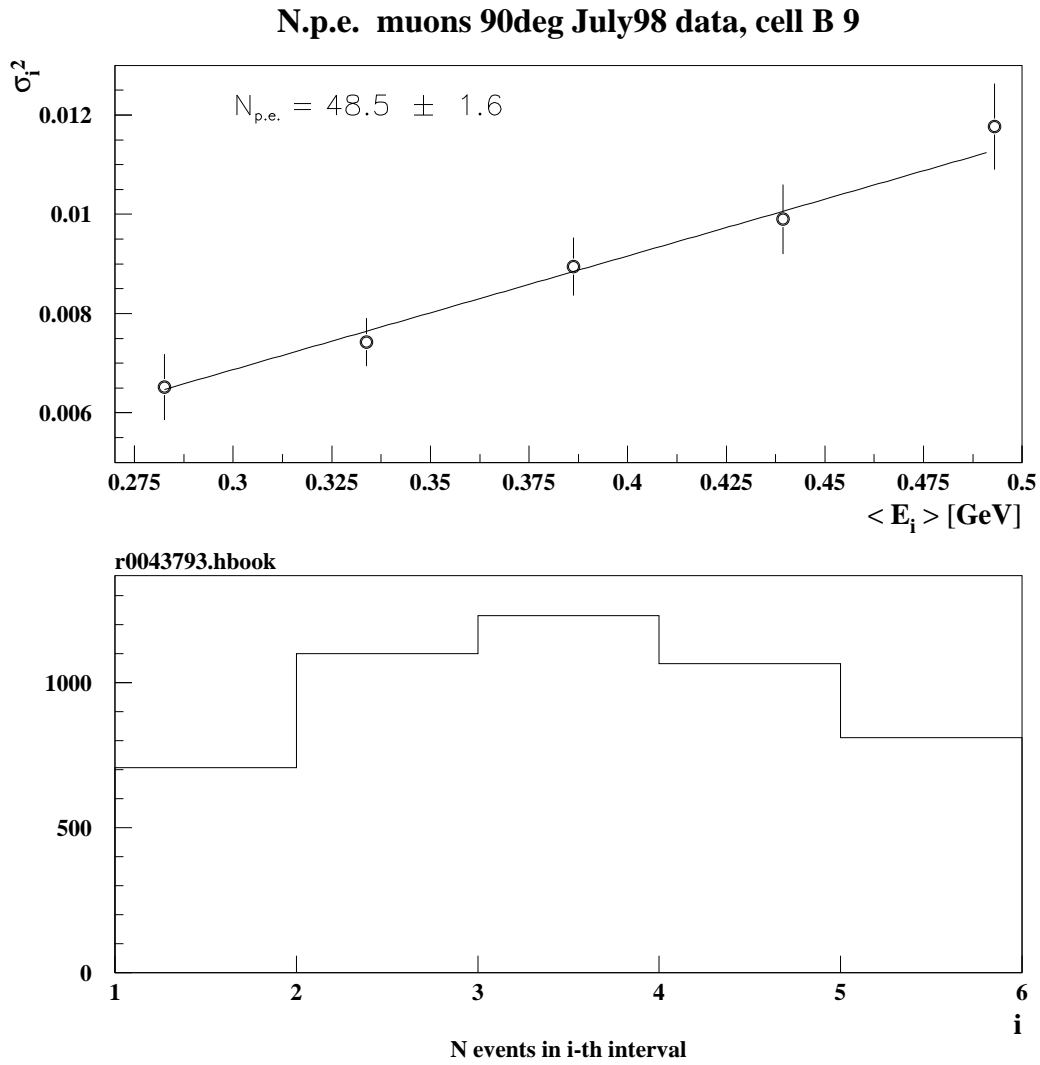


Figure 4: The number of photoelectrons per 1 GeV ($N_{p.e.}$) as the result of the fit in the cell B9 together with population of the slices.

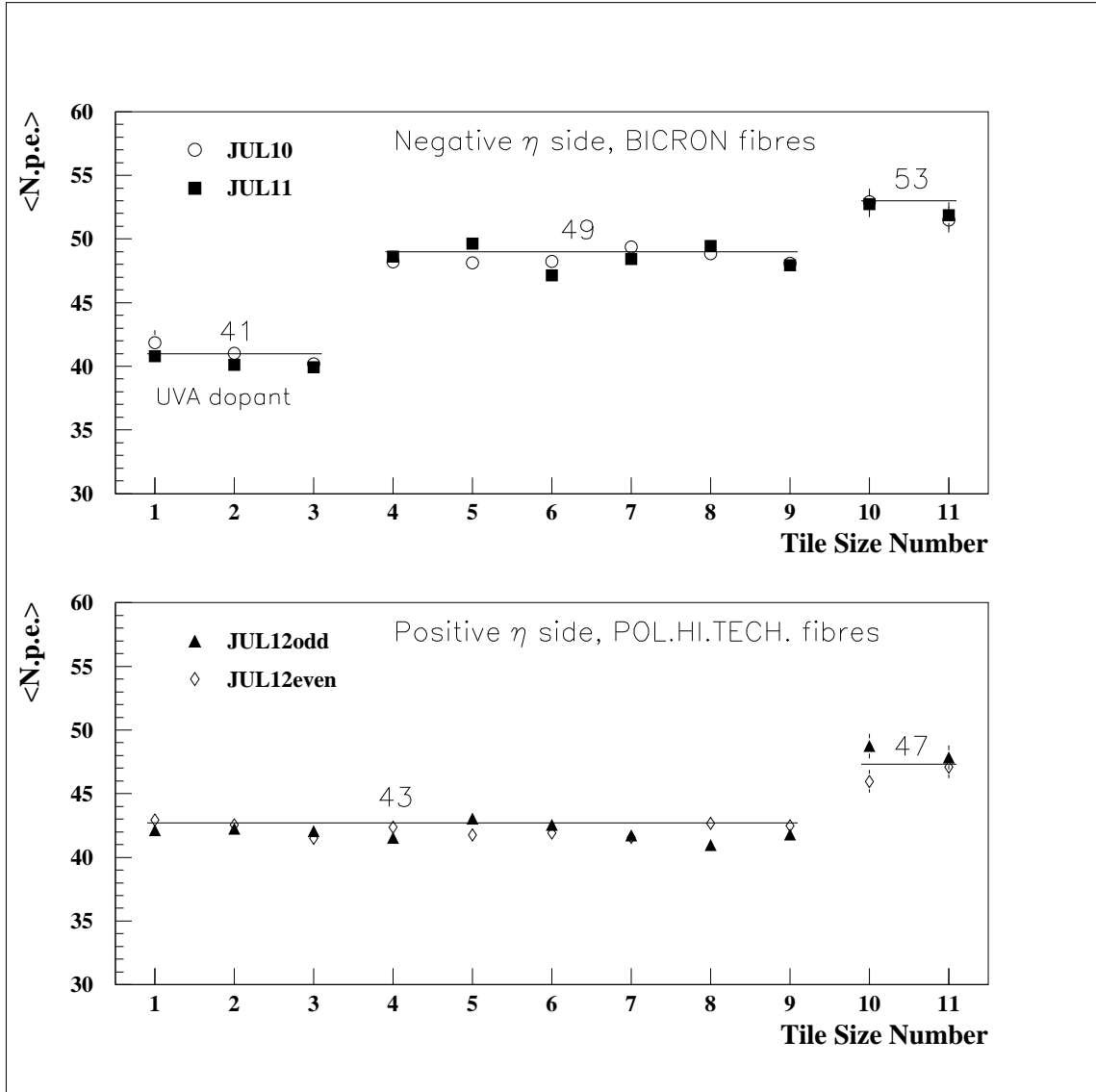


Figure 5: The average number of photoelectrons per 1 GeV ($\langle N_{p.e.} \rangle$) as a function of the tile size number (1 – 11). The negative η side is equipped with Bicron fibres and positive η side with Pol.Hi.Tech fibres. The first three tile sizes (1 – 3) on the negative η side are read by WLS fibres doped with UV absorber.

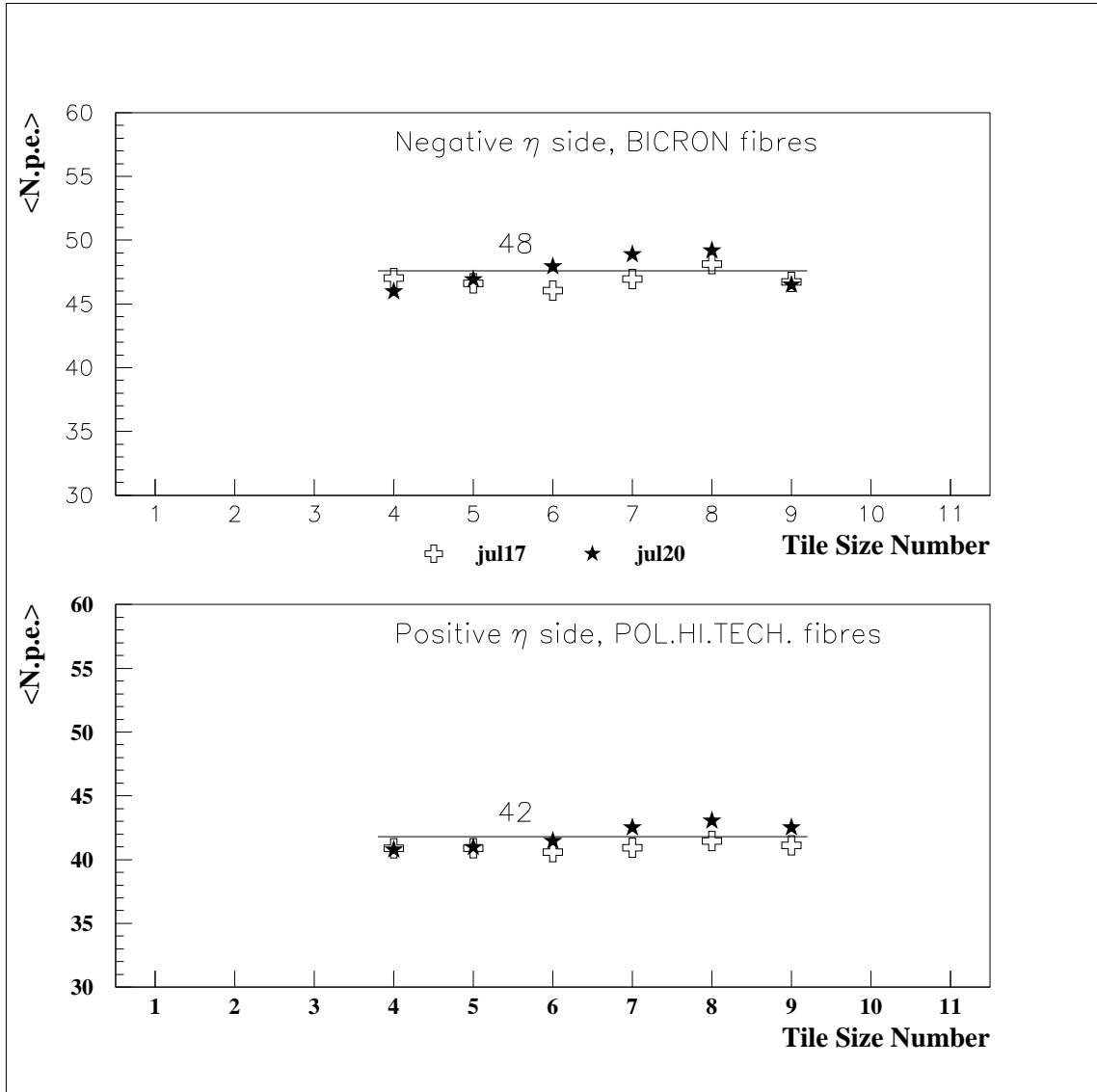


Figure 6: The number of photoelectrons per 1GeV for Sampling B, when muon energy loss is seen on both negative and positive η sides of Module 0 for the same beam particle. $N_{p.e.}$ is calculated for each cell and then averaged separately over the cells on negative and positive η sides for two data sets taken on July, 17-th (crosses) and July, 20-th (stars).